Journal of Pharmaceutical Investigation
https://doi.org/10.1007/s40005-021-00541-z

Online ISSN 2093-6214
Print ISSN 2093-5552

ORIGINAL ARTICLE

Development of clindamycin-loaded alginate/pectin/hyaluronic acid composite hydrogel film for the treatment of MRSA-infected wounds

Nurhasni Hasan[1,2] · Jiafu Cao[3] · Juho Lee[1] · Hyunwoo Kim[1] · Jin-Wook Yoo[1]

Received: 23 July 2021 / Accepted: 28 July 2021

Abstract

Purpose Methicillin-resistant *Staphylococcus aureus* (MRSA) infection on wounds possesses a high risk in increased cases of morbidity and mortality worldwide. Antibiotic-loaded composite biopolymer film wound dressings are one approach to cover the chronic wound area, promote the healing process, and create suitable healing environments. In this study, we developed clindamycin (Cly)-loaded composite biopolymer films using hydrogel-forming biopolymers, such as sodium alginate (SA), pectin (P), and hyaluronic acid (HA) for the treatment of MRSA-infected wounds.

Methods Composite films were prepared using a solvent casting method. Cly-loaded composites hydrogel films were evaluated for their physical properties (e.g., film thickness, surface morphology, pH, water vapor transmission, expansion profile, and fluid uptake), in vitro drug release, in vitro bactericidal effects, and in vivo wound healing activity in an ICR mouse model of MRSA-infected wounds.

Results Thin, transparent, and highly absorbent Cly-loaded SA-P (Cly/SA-P) and Cly-loaded SA-P-HA (Cly/SA-P-HA) film dressings were successfully prepared with good physical properties. The Cly/SA-P and Cly/SA-P-HA films exhibited drug release over 12 h under immersed conditions and potent antibacterial activity against MRSA (> 5 log reduction in bacterial viability). Furthermore, compared with the other groups, the Cly/SA-P-HA-treated group significantly accelerated the healing and re-epithelialization of wounds in a mouse model of MRSA-infected wounds. All prepared film dressings were not toxic to healthy fibroblast cells.

Conclusion Thus, the Cly-loaded composite hydrogel film prepared in this study could be a promising wound dressing for the treatment of infected cutaneous wounds.

Keywords Clindamycin · Composite hydrogel film · Sodium alginate · Pectin · Hyaluronic acid · MRSA-infected wounds

Introduction

Bacterial infection on wounds can develop into chronic wounds where the inflammation phase is prolonged, resulting in delayed wound healing and a significant burden on the healthcare system (Li et al. 2017; Hasan et al. 2019a, b). The most common bacteria that cause skin and wound infections is methicillin resistant *Staphylococcus aureus* (MRSA). Cases of infected wounds caused by this pathogen are very difficult to treat because the resistance to many antibiotics, which may increase the risk of morbidity and mortality worldwide (Dou et al. 2016; Lee et al. 2020a, b). This pathogen is also recognized as the cause of nosocomial wound infections, such as surgical site infection (SSI). SSIs are the third most common type of nosocomial infection in developed countries and cost 1.47–19.1 billion euros for surgical treatments (Leaper et al. 2004; Šiširak et al. 2010). Thus, this is a major issue, particularly in developing countries with limited resources.

Wound dressings are commonly used to cover the wound area to promote the healing process and create suitable healing environments (Kokabi et al. 2007; Huanbutta et al. 2020). For chronic wounds that produce excessive exudate,

✉ Jin-Wook Yoo
jinwook@pusan.ac.kr

1 College of Pharmacy, Pusan National University, Busan 609-735, South Korea

2 Faculty of Pharmacy, Hasanuddin University, Jl. Perintis Kemerdekaan Km 10, Makassar 90245, Republic of Indonesia

3 State Key Laboratory for Function and Applications of Medicinal Plants, Guizhou Medical University, Guiyang 550-014, China

Published online: 03 August 2021

highly absorbent and moisture-retaining dressings have been highly preferred. In this context, a thin hydrogel film dressing that facilitates autolytic debridement, conforms to the wound surface, and enables water vapor and oxygen exchange is among the popular choices. It can also absorb wound exudate to form a gel, providing a moist environment crucial for the effective healing of chronic wounds. Additionally, because of the pliable nature of film dressing, it can be easily used on body-bendable areas, such as the elbow, knee, finger joint, and hip (Moura et al. 2013; Vowden et al. 2017).

Natural polysaccharides such as sodium alginate (SA), pectin (P), and hyaluronic acid (HA), have been widely used in the fabrication of non-cross-linked film dressings. They can be used to prepare a single biopolymer or composite film (two or more polymers mixed) (Rezvanian et al. 2016; Abou-Okeil et al. 2018). However, several studies have shown that composite films can improve the mechanical properties of films; thus, composite films are preferred over single biopolymer films (Wang et al. 2010; Thu et al. 2012). Sodium alginate is a biodegradable, biocompatible, water-soluble anionic polysaccharide derived from brown algae, consisting of 1,4-linked-α-L-guluronic acid and β-D-mannuronic acid residues, which possess high absorbency and hydrogel film-forming abilities (Oshi et al. 2018; Cao et al. 2020). Furthermore, porous structures in sodium alginate hydrogels enable high-efficiency drug entrapment, followed by drug release into the wound bed (Lee et al. 2012). Sodium alginate can also promote wound healing by regulating the formation of granulation tissues, enhancing the function of macrophages and pro-inflammatory cytokines (Paul et al. 2004; Yang et al. 2009). Pectin is a natural polymer extracted from the cell walls of plants and consists of complex polysaccharide domains (e.g., homogalacturonan, rhamnogalacturonan-I, and rhamnogalacturonan-II) that play important roles in its gelling properties. Several pectin-containing hydrocolloids wound dressings have been patented and applied topically to wounds and ulcers. Natural properties of pectin such as hydrophilicity, acid environment-retention ability, and active molecule-binding capacity, make it an efficient wound dressing (e.g., absorption of wound exudates, protection against infection, and loading drugs/growth factors for enhanced healing) (Round et al. 2010; Munarin et al. 2012). Hyaluronic acid, a natural component of extracellular matrix or a polymer found naturally in the skin, is a linear polysaccharide comprising repeated disaccharide units of N-acetyl-glucosamine and D-glucuronic. Because of its unique characteristics, hyaluronic acid has been used as a wound dressing material, producing a high-water absorption and lubricant capacity, and good water retention dressings. It is also involved in wound-healing processes, such as cell migration and proliferation (Toole 2004; Neuman et al. 2015; Cho 2020). Based on the unique wound dressing properties and benefits of sodium alginate, pectin, and hyaluronic acid in promoting healing mentioned above, we hypothesized that the composite hydrogel film prepared from these polymers would produce a promising wound dressing for the treatment of cutaneous wounds.

However, in the case of chronic wound infection, wound dressings are not sufficient to accelerate the healing process. Therefore, a combination of wound dressings and antibiotics is required. Clindamycin (Cly) is a semisynthetic derivative of lincomycin that exhibit antibacterial activity by inhibiting protein synthesis and ribosomal translocation (Spížek et al. 2017). Because of the effective antibacterial activity of Cly against several aerobic gram-positive cocci (e.g., *Staphylococcus aureus*, streptococci) and anaerobes (e.g., *Bacteroides* spp. and *Clostridium perfringens*), it has been widely used for the treatment of a variety of skin and soft tissues infections (Spížek et al. 2004; Stein et al. 2016). Moreover, several studies have reported the efficacy of Cly against resistant pathogen, such as MRSA (Hasan et al. 2019a, b; Vivekanandan et al. 2020).

In the present study, we developed Cly-loaded composite hydrogel films consisting of SA, P, and HA to treat MRSA-infected wounds. After evaluating their physical properties, films were tested for in vitro drug release, in vitro bactericidal effects, and in vivo wound-healing activity in an ICR mouse model of MRSA-infected wounds.

Materials and methods

Materials

SA (MW 80–120 kDa with a mannuronate/guluronate value of 1.56), Mayer's hematoxylin, eosin-Y disodium salt, 2,2,2-tribromoethanol and tert-amyl alcohol (2-methyl-2-butanol) (Avertin anesthesia components), tetrazolium dye 3-(4,5-di-methylthiazol-2-yl)-2,5-diphenyltetrazolium bromide (MTT), and dimethyl sulfoxide (DMSO) were purchased from Sigma-Aldrich (St. Louis, Missouri, USA). P from citrus plants was purchased from Yakuri (Kyoto, Japan). Oligo-HA (MW 0.5–10.1 kDa) was purchased from SK Bioland (Cheonan, Korea). The Pierce™ BCA Protein Assay Kit was purchased from Thermo Fisher Scientific Korea (Seoul, Korea). Bacto™ tryptic soy broth (TSB) medium and peptone were purchased from BD Biosciences (San Jose, California, USA). The LIVE/DEAD® Baclight™ bacterial viability kit (Molecular Probes) was purchased from Life Technologies (Eugene, Oregon, USA). Roswell Park Memorial Institute (RPMI) 1640 medium, trypsin, fetal bovine serum (FBS), and penicillin–streptomycin were procured from Hyclone, Thermo Fisher Scientific Inc. (Waltham, Massachusetts, USA). Adhesive tape (Micropore) and Tegaderm™ (transparent dressing) were purchased from

3 M Health Care (St Paul, Minnesota, USA). Phosphate-buffered saline (PBS) 20 × was purchased from Biosesang (Seoul, South Korea). All other reagents and solvents were of analytical grade.

Film preparation

Cly-loaded hydrogel and an aqueous hydrogel (blank) were prepared using the solvent casting method. SA composite films were prepared in equal mass fractions (1:1) with P (SA-P) or ratio of 1:1:0.5 with P-HA (SA-P-HA). Table 1 shows the composition of the gels used for film casting. The gels for casting films were prepared by dissolving the polymers in distilled water and stirring continuously at 1000 rpm for 2–3 h at 40 °C. These homogenized gels were added to glycerin, sonicated for at least 1 h, and then left at room temperature to eliminate any remaining air bubbles. The blank films were dry cast by pouring 20 g of the gel into a plastic Petri dish (d = 90 mm) and drying in an oven at 45 °C for 36 h. The drug-loaded polymeric gels were prepared by incorporating 5 mL of an aqueous solution of Cly (10 mg/g) into the gels to achieve a final drug concentration of 1 wt.%. These drug-loaded gels were oven-dried, as described previously for blank gels, and stored in a desiccator.

Film thickness and pH

Surface morphology

A field emission scanning electron microscope (FE-SEM) was used to examine the surface morphology of the films (FE-SEM, S4800, Hitachi, Japan). Under vacuum, samples (0.8×0.8 cm^2) were mounted on double-sided carbon tape and coated with platinum for 2 min. The samples were examined with an FE-SEM at an acceleration voltage of 1–5 kV.

Film thickness

A digital outside micrometer (Bluebird Multinational Co., Japan, sensitivity = 0.001 mm) was used to measure the thickness of the films at five different locations (one at the center and four near the edges). For each film, this test was performed in triplicate, and the mean values were recorded. In addition, SEM images were used to evaluate film thickness.

Table 1 Film composition

Film composition	SA-P	Cly/SA-P	SA-P-HA	Cly/SA-P-HA
Clindamycin HCl/Cly	–	1.00	–	1.00
Sodium alginate/SA (g)	2.50	2.50	2.50	2.50
Pectin/P (g)	2.50	2.5	2.50	2.50
Hyaluronic acid/HA (g)	–	–	1.25	1.25
Glycerin (g)	2.50	2.50	3.12	3.12
Distilled water (g)	92.50	91.50	90.63	89.63

pH

All films were suspended in distilled water at a 1:100 (w/v) ratio and stored at room temperature for 24 h. pH was measured using a pH meter. These measurements were performed after 24 h at pH 7.

Water vapor transmission (WVT)

The measurement of WVT rate of the films was measured according to a previously reported method, with slight modifications (Thu et al. 2012). A circular template with a diameter of 30 mm was used to cut the films. The cut films were secured to the brim of a 6 mL glass vial (30 mm in diameter) containing 3 g of fused calcium chloride as a desiccant. The vial was weighed and stored in a desiccator at 25 °C with a relative humidity of 84% and the moisture was controlled with a saturated potassium chloride solution. The vial was removed from the desiccator and weighed every 1 h for 24 h. The WVT rate was calculated by plotting the slope of the amount of water gain versus time at each time interval. The experiment was repeated three times, and the average values were computed using the following equation:

$$WVT = \frac{WT}{S}$$

where W is the weight of the water, T is the number of hours in the experiment, and S is the exposed surface area of the film.

Film expansion profile

Gelatin solution with a concentration of 4% w/v was prepared by dissolving 4 g of gelatin powder in 100 mL of distilled water at 70 °C with constant stirring at 700 rpm. Then, 20 g of this solution was poured into a Petri dish and incubated overnight at 25 °C to form a gel. Subsequently, each drug-loaded film was cut into a circular shape of a specific size (22 mm in diameter) and placed in the center of the gelatin gel. The diameters of the films were measured at predetermined time intervals. The test was repeated three times for each formulation, and the mean value was used to calculate the expansion behavior using the equation below:

$$E = \frac{Dt - Do}{Do} \times 100$$

where E is the expansion ratio, D_t is the film's diameter after expansion, and D_0 is the film's diameter before expansion.

Fluid uptake study

The ability of the films to uptake simulated wound fluid (SWF) was measured as previously described, with some modifications (Etxabide et al. 2017). SWF comprises 0.1 g of peptone and 0.85 g of NaCl in 100 mL of distilled water mixed with FBS at a ratio of 1:1 (Choi et al. 2020). The swelling weights of SA-P, Cly/SA-P, SA-P–HA, and Cly/SA-P-HA films were measured at various time points (10, 30, 60 and 120 min). First, four dried films (2×2 cm^2) were weighed and used as the control ($t = 0$). Second, after draining the remaining drops with a paper towel, the films were completely immersed in 10 mL of PBS and weighed at specified times. The percentage of weight gain compared to the control was calculated, and the mean values were obtained for each time point. A plot of the percentage swelling index versus time was used to calculate the fluid uptake, according to the following equation:

$$\text{Fluid uptake}\,(\%) = \frac{Wt - Wo}{Wt} \times 100$$

where W_0 and W_t are the weights of the dry and swollen polymers measured at different time periods, respectively.

Drug loading

Cly entrapped in the films was determined using high performance liquid chromatography (HPLC, Shimadzu, Kyoto, Japan). The HPLC (Shimadzu, Kyoto, Japan) peak and retention time analysis were measured. The HPLC system was equipped with an LC-20AT liquid chromatograph, SPD-20A prominence UV/Vis detector, CT-20A prominence column oven, DGU-20ASR degassing unit, and SIL-20 prominence auto sampler. Cly salt and base were dissolved in mobile phase consisted of acetonitrile and phosphate buffer (pH 3.0; 52:48, v/v), filtered through a 0.45 µm nylon membrane, and pumped at a flow rate of 1.0 mL/min. A VDSpher® PUR 100 C18-M-SE columns (5 µm, 250 × 4.6 mm, VDS Optilab, Germany) was used. The elution was monitored at 210 nm with an injection volume of 20 µL.

A specific amount of Cly/SA-P and Cly/SA-P-HA films were dissolved in distilled water, sonicated for 4 h and centrifuged at 20,000 × *g* for 5 min. The supernatant was diluted to a suitable dilution with a mobile phase, and each sample (100 µL) was transferred to an HPLC autosampler cell and measured under chromatographic conditions described above. A Cly standard stock solution was prepared by dissolving the Cly base in the mobile phase. In the concentration range of 0.004 to 1 mg/mL, the linear correlation between peak area and Cly concentration ($R^2 = 0.9998$) was obtained. Each sample was prepared in triplicate.

In vitro drug release

The Cly release of Cly/SA-P and Cly/SA-P-HA films was evaluated in PBS with pH 7.4 at 37 °C under immersed condition. Films (100 mg) were added to 5 mL of the release medium and incubated in a shaking water bath (37 °C) with mild stirring. At predetermined time intervals, 100 µL of supernatant were withdrawn, and volumes were prepared with fresh buffer solution. The supernatant containing Cly released from the films were analyzed using HPLC as described in Sect. Drug loading.

In vitro antibacterial activity

To evaluate the antibacterial activity of Cly/SA-P and Cly/SA-P-HA films, a colony-forming unit (CFU) assay was employed to count the number of viable bacteria. The bacterial strain used in this study was MRSA (USA300) FPR3757 (GenBank accession no.: NC_00793). The bacteria were inoculated on TSB agar and cultured overnight at 37 °C to the mid-exponential phase (10^8 CFU/mL). The resulting bacterial suspension was centrifuged at 8000 × *g* for 15 min. The pellet was resuspended in sterile PBS and adjusted to an appropriate concentration. A total of 100 µL of the bacterial suspension (final concentration 10^7 CFU/mL) was incubated with 2 mL of TSB medium in a microtube. Then, the films were immersed in media containing bacteria at a final concentration of approximately 2–3 mg/mL. Bacteria in sterile PBS were used as controls. All samples were incubated at 37 °C for 24 h in a shaking incubator, centrifuged at 100 × *g*, and washed twice with 0.85% NaCl. For bacterial viability (CFU measurement), the bacterial suspensions were diluted in PBS (10^{-1} to 10^{-8}). A 200 µL aliquot of each dilution was plated on TSB agar medium and incubated at 37 °C overnight. The number of colonies was counted as the number of viable bacteria at plating time. Bacterial suspensions were stained with the LIVE/DEAD® Baclight™ bacterial viability kit reagents according to the manufacturer's protocol for the confocal study. The samples were examined using confocal microscope (Fluoview FV10i, Olympus Corporation, Tokyo, Japan) to distinguish between live and dead bacteria. Bacteria stained green with SYTO-9 at Ex/Em wavelengths of 539/570–620 nm were considered viable/live, while those stained red with propidium iodide (PI) at Ex/Em wavelengths of 470/490–540 nm were considered dead.

In vitro cytotoxicity study

L929 mouse fibroblasts from the Korean Cell Line Bank (KCLB, Seoul, Korea) were cultured in RPMI medium supplemented with 10% (v/v) FBS and antibiotics (100 IU/mL penicillin G sodium and 100 µg/mL streptomycin sulfate). Cells were incubated overnight at 37 °C in an incubator with 5% CO_2 and a humidified atmosphere. Cells were seeded at a density of 2×10^4 cells per well in a 96-well plate (SPL Life Sciences Co., Gyeonggi-do, South Korea) and incubated for 24 h. The media were then replaced with fresh media containing SA-P, Cly/SA-P, SA-P-HA, or Cly/SA-P-HA films at increasing concentrations (10, 20, 40 mg/mL) and incubated for 24 h. Free drug (Cly HCl) at a concentration of 1 mg/mL was also tested. After incubation, each well received a standard MTT solution in sterile PBS was incubated for 2 h. The MTT solution was then removed and 150 µL of DMSO was added to each well. The absorbance measured at 540 nm was proportional to the concentration of viable cells in each well. Untreated cells were used as the control. The data are expressed as the mean ± standard deviations of eight replicates (n = 8). The cell viability was calculated using the following equation (Banna et al. 2018):

$$\text{Cell viability}(\%) = \frac{Absorbance(treated\ cells)}{Absorbance(control\ cells)} \times 100$$

Protein adsorption

The film was cut (size 2×2 cm^2) and immersed in 4 mL of PBS buffer solution containing bovine serum albumin (BSA). The solution was shaken at 100 rpm during incubation. After 24 h, the samples were gently removed and rinsed five times with PBS. Next, the samples were placed in a 6-well plate containing aqueous sodium dodecyl sulfate solution (1%) and shaken for 1 h to remove adsorbed proteins on the surface. The Pierce™ BCA Protein Assay Kit was used to determine the protein content of each sample according to the manufacture's protocol. A microplate reader was used to measure the absorption at 562 nm.

In vivo wound-healing activity

Male ICR mice (7–8 weeks old, Samtako Bio Korea) were used as the animal model. All animal experiments were performed in accordance with the regulations of Korean legislation on animal studies and were approved by the Ethical Scientific Committee of Pusan National University. Before introducing wounds to the dorsal area, the mice were anesthetized intraperitoneally using Avertin at a dose of 250 mg/kg. The dorsal hair was shaved with an electric razor, and dorsal skin was excised with an 8 mm biopsy punch to create full-thickness wounds. Then, a bacterial suspension (60 µL) containing 1×10^7 MRSA (USA300) FPR3757 was inoculated to induce infection in the wound. The SA-P, Cly/SA-P, SA-P-HA, and Cly/SA-P-HA films were topically applied (20 mg) at day 2 post-injury site when signs of infection were observed. Each wound was covered with sterile gauze. Untreated mice were used as the control. The gauze on the wound lesions was replaced with new gauze at predetermined time. Photographs of the wounds were taken to observe gross visual wound healing based on the wound area not covered by migrating epithelial cells. ImageJ (National Institutes of Health, Bethesda, Maryland) was used to determine the reduction in wound size, which was calculated as follows:

$$\text{Wound size reduction}(\%) = \frac{Wt}{Wo} \times 100$$

where W_0 is the wound area at initial time 0 and W_t is the wound area at time t.

Histological analysis

Cross-sectional full-thickness skin specimen and deep granulation tissue were collected on day 6 post-injury and the last day of the experiment. Full wound areas were excised, fixed in 10% formaldehyde for 24 h, and embedded in paraffin. Five-micron thick, vertical sections were fixed on glass slides and processed using hematoxylin and eosin (H&E) stains to evaluate the morphology of the skin. The slides were examined using light microscopy (Olympus BX53, Olympus Corporation, Tokyo, Japan), and images were digitally captured at a pixel resolution of 1360×1024 with an Olympus DP70 digital camera.

Statistical analysis

Statistical analyses were performed using a one-way analysis of variance (ANOVA) followed by Tukey's multiple comparison tests or using an unpaired *t*-test in GraphPad Prism 5.0 (GraphPad Software, La Jolla, CA, USA). In cases of significant deviations from the normality, the nonparametric Mann–Whitney U test was performed instead of the *t*-test to compare the distributions of the two unpaired groups. Statistical significance was set at ***$P < 0.001$. Data are presented as the mean ± standard deviations.

Results and discussion

Film preparation

In this study, our aim was to develop Cly-loaded composite biopolymer films as potential dressings to treat

MRSA-infected wounds. Hydrogel-forming biopolymers, including SA, P, and HA, were used to fabricate two different composite films. Non-cross-linked films made by mixing two polymers (SA-P) and three polymers (SA-P-HA) were prepared and compared. Polymer concentrations of 5–6.25 (wt.%) were chosen to produce hydrogels which were easy to pour and devoid of lumps. As a result, the blank and drug (Cly)-loaded hydrogel could be formed into a film after the addition of glycerin as a plasticizer, followed by drying in an oven at 45 °C for 36 h. Each dried film was produced by pouring 20 g of hydrogel into a petri dish as a film mold. This weight was ideal for casting a thin film (not too thick or too thin). Choi et al. prepared a nitric oxide-releasing chitosan film by casting 20 g of the gel solution into a petri dish. The result was a thin and flexible film which was promising as wound dressing for the treatment of MRSA biofilm-infected wounds (Choi et al. 2020). Furthermore, the blank films and Cly-loaded composite films were smooth and flexible in texture. The addition of glycerin also helped increase film flexibility and made it easier to remove from the mold. Therefore, following the optimization of film formulations using the appropriate ratio of each polymer and technique, a flexible and non-brittle film dressing was successfully prepared.

Characterization of the films

Surface morphology and thickness of the film

As shown in Fig. 1a, all films (SA-P, Cly/SA-P, SA-P-HA, and Cly/SA-P-HA) were translucent, which can help to inspect the wound beds without having to remove the

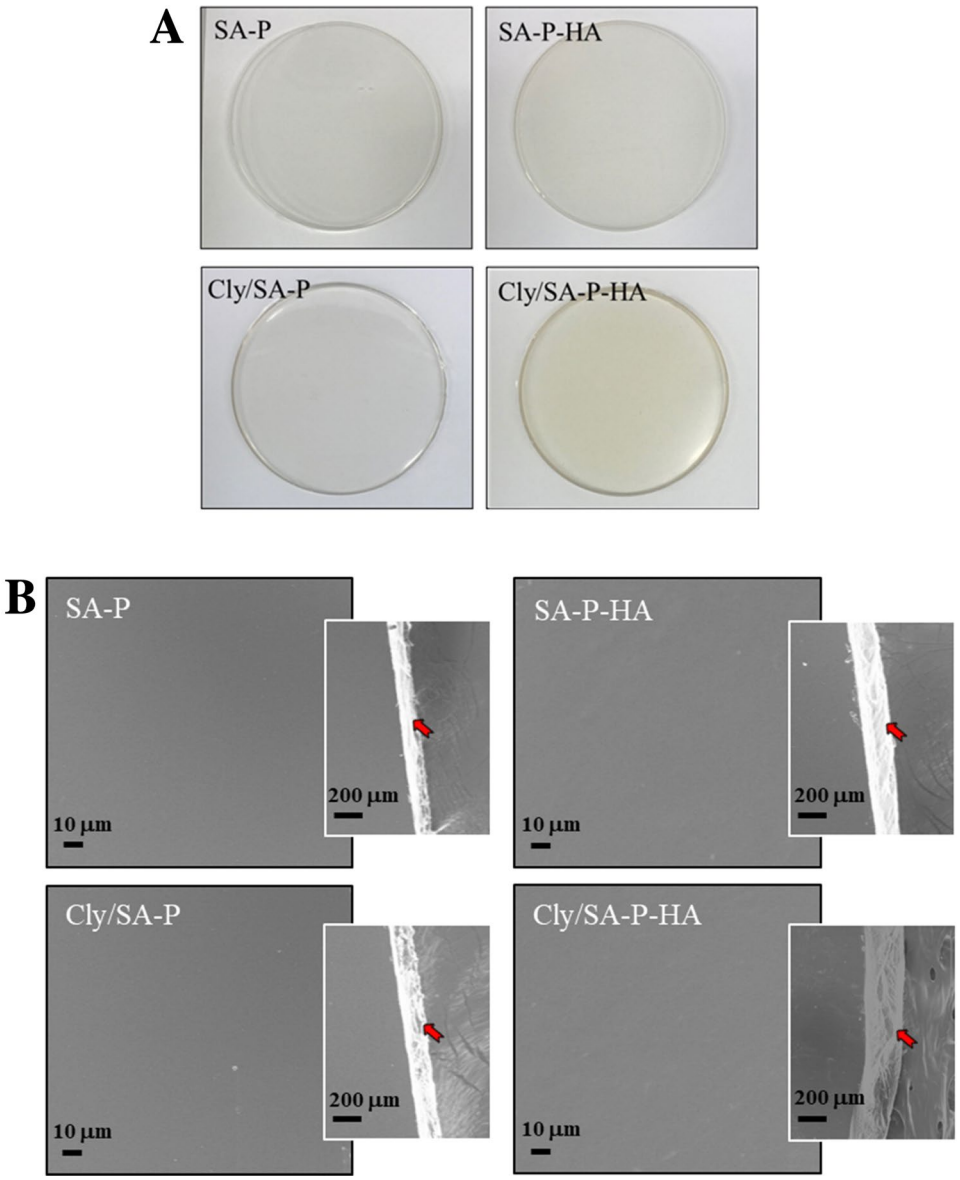

Fig. 1 **a** Photographs of films. **b** Scanning electron microscopy images of films

dressing when these films were applied to the wound. SEM was used to observe potential drug crystals on the surface of the films. As shown in Fig. 1b, SA-P, Cly/SA-P, SA-P-HA, and Cly/SA-P-HA films had a smooth surface and homogeneity, indicating that the addition of Cly did not affect the surface morphology of the composite films. The thickness of the films could also be observed from the side image of the film using SEM (Fig. 1b, small image). As shown in the SEM image, the blank films (SA-P and SA-P-HA) were thinner than the Cly-loaded composite films (Cly/SA-P and Cly/SA-P-HA). Thus, the addition of the drug directly affected the thickness of the film. Additionally, composite films from three mixed polymers (SA-P-HA) were thicker than those with two mixed polymers (SA-P), indicating that the thickness of the composite film was directly influenced by the polymer concentration in the film. The observation of film thickness using SEM images was in line with the measurement of the mean thickness of the films, as shown in Table 2. The mean thickness of SA-P, Cly/SA-P, SA-P-HA, and Cly/SA-P-HA films was 0.18 ± 0.01, 0.21 ± 0.05, 0.21 ± 0.01, and 0.25 ± 0.02 mm, respectively. This range of film thickness (0.18–0.25 mm) was ideal for wound dressing. The film was not too thin, making it easily broken or curled, or too thick, making it stiff and difficult to apply to the bendable areas of the body.

pH, drug loading, and loading efficiency

As presented in Table 2, the pH of the composite films from the two mixed polymers (SA-P) was slightly higher than that of the three mixed polymers (SA-P-HA). The pH values of SA-P, Cly/SA-P, SA-P-HA, and Cly/SA-P-HA films were 5.51, 5.25, 4.49, and 4.45, respectively. The HA present in the three mixed polymers contributed to the slightly low pH value of the resulted film. However, the pH values of all films presented in this study met the requirements of the ideal pH for wound dressing. It is necessary to adjust the pH of dressings based on the pH in the wound bed area. It has been reported that as the wound heals, the pH value shifts to neutral and becomes acidic (Tsukada 1992).

There were no significant differences in the drug loading of Cly/SA-P and Cly/SA-P-HA films. The drug loading levels of Cly/SA-P and Cly/SA-P-HA films were 12.11 ± 0.19 wt.% and 10.15 ± 0.01 wt.%, respectively. Furthermore, the loading efficiencies of Cly/SA-P and Cly/SA-P-HA films were 99.5 and 99.6%, respectively. Thus, the results suggested that the polymer concentration did not directly affect the drug loading or loading efficiency.

WVT rate

An ideal wound dressing should, in general, provide an optimal rate of moisture transmission to prevent exudate accumulation and excessive dehydration at the wound site; thus, measuring WVT rate is important (Rezvanian et al. 2016). As shown in Fig. 2a, the WVT rates of SA-P, Cly/SA-P, SA-P-HA, and Cly/SA-P-HA films were 1153, 1232, 1444, and 1501 g/m^2/24 h, respectively. Based on chronic wounds (such as burn and granulating wounds), the WVT rate falls with a range between 279 and 5138 g/m^2/24 h (Lamke et al. 1977); therefore, all films used in this study were permeable to water vapor and able to keep the wound site moist and being ideal for low to medium levels of wound exudate. Moreover, excessive dehydration can be also avoided. The results also showed that the WVT rates of composite films from the two mixed polymers (SA-P) were significantly higher (***$P < 0.001$) than those of the three mixed polymers (SA-P-HA) due to the difference in the film thickness. The rate of water molecule diffusion across the films was affected by the film thickness. Accordingly, the WVT rate of a hydrophilic biopolymer film is determined by the length of the moisture path (Parris et al. 1997). Therefore, the results suggested that all films could maintain high humidity in the wound bed, creating a moist environment that is crucial for aiding healing processes such as enhanced cell migration and re-epithelialization (Mohamad et al. 2014).

Film expansion ratio

Wound exudates are absorbed into the film matrix when a dried film comes into contact with a moist wound surface. This causes the film to hydrate, expand, and eventually turn into a gel on the wound surface. The purpose of this film expansion study was to determine the rate of expansion (or hydration) of the film dressings. The gelatin model was used to simulate the moist wound surface environment (Matthews

Table 2 Thickness, pH, drug loading, and loading efficiency

Film-based wound dressing	Thickness (mm)	pH	Drug loading (wt.%)	LE (%)
SA-P	0.18 ± 0.01	5.51 ± 0.06	–	–
Cly/SA-P	0.21 ± 0.05	5.25 ± 0.05	12.11 ± 0.19	99.5 ± 1.60
SA-P-HA	0.21 ± 0.01	4.49 ± 0.11	–	–
Cly/SA-P-HA	0.25 ± 0.02	4.45 ± 0.04	10.15 ± 0.01	99.6 ± 0.04

Values are expressed as mean averages ± standard deviations of three different batch of films

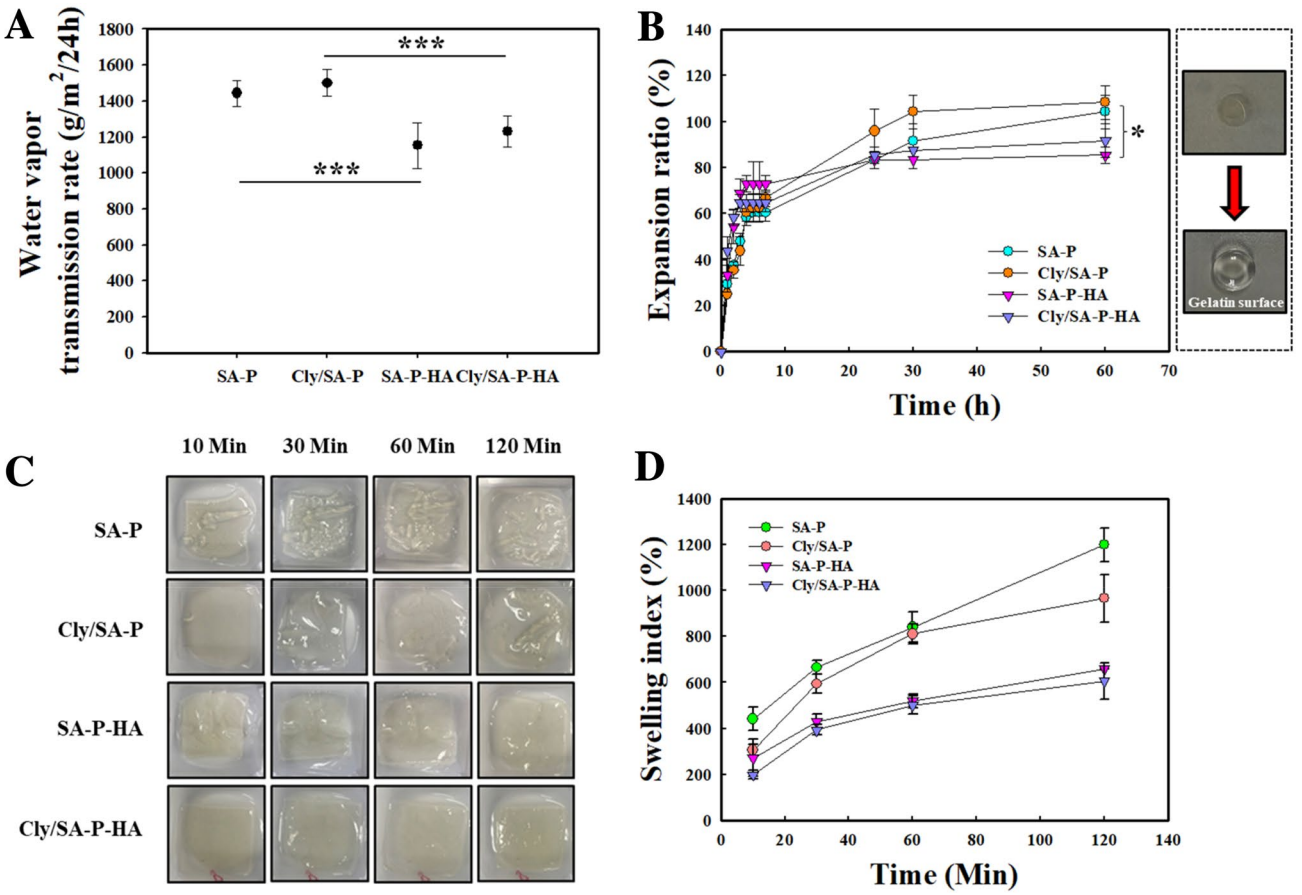

Fig. 2 **a** Water vapor transmission rate of films. **b** Expansion ratio of films. Swelling of films **c** Macroscopic images of film swelling, and **d** Swelling index of the films. Data are presented as means ± standard deviations; $n = 3$

et al. 2005). Figure 2b depicts the percentage increase in the expansion of the drug-loaded films as a function of time. Following the slow hydration process on the gelatin surface, the disk-shaped films expanded in all directions and eventually transformed into gels (Fig. 2b, side box). After 2 h, the hydration rate was slower in the composite film containing three mixed polymers (SA-P-HA and Cly/SA-P-HA), than in the composite films containing two mixed polymers (SA-P and Cly/SA-P). SA-P-HA and Cly/SA-P-HA films had the greatest expansion, most likely caused by their low mechanical strength. After 4 h, SA-P-HA and Cly/SA-P-HA films gradually expanded to 54 and 58% of their initial sizes, respectively. The rehydrated composite films from two mixed polymers (SA-P and Cly/SA-P) had the lowest apparent viscosity; thus, they expanded faster over the gelatin surface, resulting in a higher expansion ratio up to 7 h. Therefore, Cly/SA-P film may be beneficial for wounds with low suppuration. Furthermore, after 30 h, the films expanded by 83% of their initial size. The composite film containing three mixed polymers (SA-P-HA and Cly/SA-P-HA) exhibited a slower expansion rate from their initial size up to 24 h. This indicated that SA-P-HA and Cly/SA-P-HA films could retain their shape during dressing application while undergoing a hydrating process to provide a moist environment on the wound bed. For heavy exudative wounds, a wound dressing that maintain its structure and shape for a longer period is preferable (Rezvanian et al. 2016). The expansion values of all films did not differ significantly after 24 h.

Water uptake study

Water uptake by the film is an important property in skin tissue engineering applications, as wounds must be kept moist and excess exudates removed (Kim et al. 2015). When the composite hydrogel film comes into contact with the wound exudate, it forms a hydrogel. Therefore, the water uptake ability was investigated to determine the maximum swelling condition. The swelling of the Cly-loaded composite hydrogel films was also caused by the absorption of the SWF-aided drug release. The composite films from two mixed polymers (SA-P and Cly/SA-P) rapidly absorbed SWF (Fig. 2c), up to 840 and 810% of their mass in SWF within 60 min, respectively (Fig. 2d). Following the initial rapid absorption of SWF, the fluid uptake by SA-P and Cly/SA-P continued

to increase, reaching approximately 1198 and 966%, respectively, at 120 min with no further significant fluid absorption observed thereafter. In contrast, the composite films from the three mixed polymers (SA-P-HA and Cly/SA-P-HA) exhibited slower water uptake (Fig. 2c). SA-P-HA and Cly/SA-P-HA films absorbed up to 519 and 501% of their mass, respectively, in SWF within 60 min (Fig. 2d). Following the initial rapid absorption of SWF, the fluid uptake by SA-P-HA and Cly/SA-P-HA films slowed, reaching approximately 660 and 605%, respectively, at 120 min. Combining three polymers, SA, P, and HA, may contribute to the mechanical properties of the composite hydrogel films, thus affecting their water uptake ability. However, the results still suggested that all films had a good swelling index because of the SA polymer. The hydrogen bonds formed between alginate and water molecules enabled the SWF to become trapped in the intermolecular space of the hydrogel structure. After the intermolecular space is filled with SWF, no more fluid can be absorbed, thereby reaching the maximum swollen condition (Lee et al. 2019; Hasan et al. 2021) (Fig. 2d).

In vitro release study

The in vitro drug release was evaluated in PBS as a release medium under immersed conditions to mimick the infected-wounds condition. Infected-wounds normally produce high amount of wound exudate (Choi et al. 2020); thus, the immersed condition represents infected-wounds with a high amount of exudate in which the Cly/SA-P and Cly/SA-P-HA films swell rapidly, resulting in slightly increased drug release rate. The in vitro release of Cly from the composite hydrogel films is shown in Fig. 3. Cly was burst released from Cly/SA-P and Cly/SA-P-HA films within the first 4 h, followed by a gradual release over the next 10 h. In the first 2 h, Cly was released slightly faster from the Cly/SA-P film than from the Cly/SA-P-HA film. As much as 88.92% of the Cly was released from the Cly/SA-P film within the first 2 h, followed by 99.*99%* at 12 h. However, Cly was released from the Cly/SA-P-HA film at slightly slower rates, achieving 77.51% release at 2 h and reaching 96.65% release in 12 h. The slight difference in release profile might be due to the difference in water uptake ability between Cly/SA-P and Cly/SA-P-HA films. In which, Cly/SA-P film exhibited faster water uptake than Cly/SA-P-HA film. Thus, Cly was released faster from the Cly/SA-P film than the Cly/SA-P-HA film. Based on the release profile, the application of these Cly-loaded composite hydrogel films to the MRSA-infected wounds was set at once daily. The application of wound dressing once daily can help promote wound healing as compared to that of dressing that requires many times daily dressing changes. Frequent dressing changes have been linked to an increased risk of wound sepsis and delayed wound healing (Wynne et al. 2004).

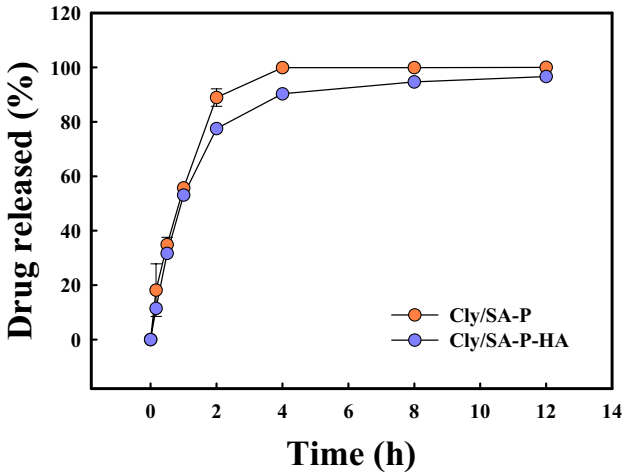

Fig. 3 In vitro release profile of films. All samples were suspended in PBS with pH 7.4 at 37 °C; data are presented as means ± standard deviations; $n = 3$

In vitro antibacterial study

Before evaluating the effectiveness of the Cly-loaded composite films (Cly/SA-P and Cly/SA-P-HA) in eradicating infection and accelerating wound healing in in vivo MRSA-infected wounds, the in vitro antibacterial activity against MRSA was evaluated by confocal microscopy and CFU measurements. Blank films (SA-P and SA-P-HA) were used as controls. Confocal microscopy was used to observe the fluorescent images of live and dead bacteria to examine the reduction in MRSA viability (Fig. 4a). The reagents-stained live cells exhibited green fluorescence (SYTO-9), and reagent-stained dead cells exhibited red fluorescence emitted by PI. SYTO-9 can pass through all bacterial membranes, whereas PI can only pass-through cells with damaged membranes (Nurhasni et al. 2015). Both Cly/SA and Cly/SA-P-HA films showed significant antibacterial effects against MRSA, as indicated by the significant intensity of red fluorescence. In contrast, the blank films (SA-P and SA-P-HA) showed no antibacterial activity against MRSA, as indicated by the green fluorescence intensity. These results agreed with the macroscopic images of the bacterial density observed in the TSB medium, in which both Cly/SA-P and Cly/SA-P-HA films exhibited clear medium and indicated that both films significantly killed bacteria (Fig. 4b). However, the blank films (SA-P and SA-P-HA) showed a high density of the TSB medium. Furthermore, we performed a CFU assay to confirm the ability of the Cly/SA-P and Cly/SA-P-HA films in the reduction of MRSA viability. As shown in Fig. 4c, similar to the results obtained of confocal microscopy and macroscopic images of the bacterial density, the blank films revealed no reduction in bacterial viability after 24 h of incubation. In contrast, the Cly/SA-P

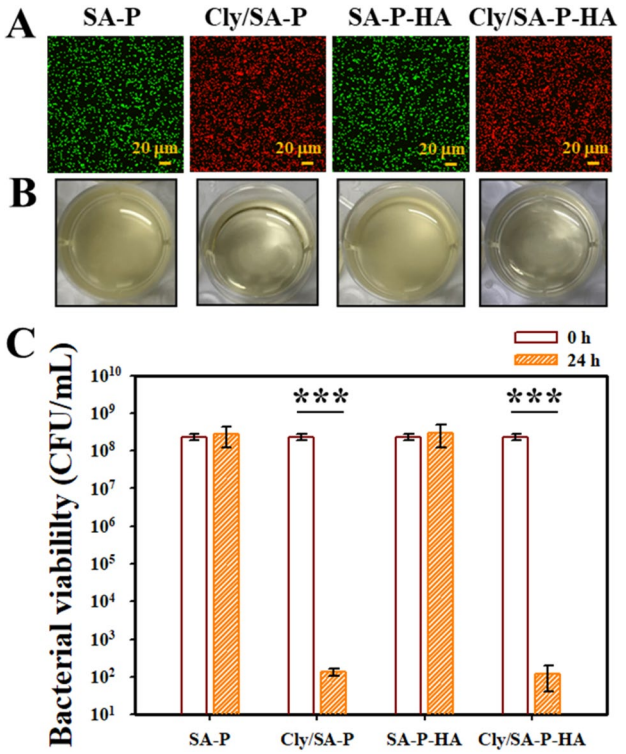

Fig. 4 In vitro antibacterial activity. **a** Confocal microscopy images after 24 h of treatment with the film. SYTO-9 fluorescence (green) indicates the intact membrane of bacteria, PI fluorescence (red) indicates membrane destruction and cell death. Bars represent 20 µm. **b** Macroscopic images of bacterial density in the TSB medium. **c** Bacterial viability (CFU/mL), values data are expressed as means ± standard deviations ($n = 3$)

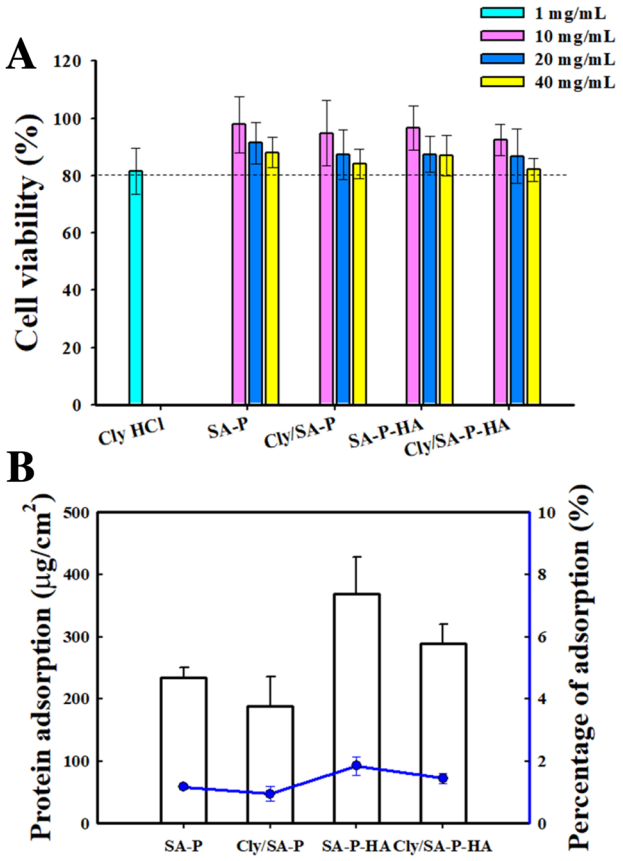

Fig. 5 **a** Viability (%) of L929 mouse fibroblast cells following 24 h exposure to films at different concentrations ($n = 8$). **b** Protein adsorption of films

and Cly/SA-P-HA films (containing 300 µg Cly/mg in each film) reduced bacterial viability by > 5 log (approximately 99.999% of killing) against MRSA. Thus, these results suggested that both Cly-loaded composite hydrogel films, from two mixed polymers (SA-P) and three mixed polymers (SA-P-HA), have similar potent antibacterial activity against MRSA. The potent antibacterial activity was solely contributed by drug loaded in the composite hydrogel films. Cly is an FDA-approved antibiotic for the treatment of MRSA bacterial infections and is well known to kill MRSA by inhibiting protein synthesis and ribosomal translocation (Martínez-Aguilar et al. 2003; Spížek et al. 2017). The polymers themselves do not contribute to antibacterial activity.

In vitro cytotoxicity study

Cytotoxicity is a critical factor in determining the safety of biomedical materials. Healthy L929 mammalian fibroblast cells were used to assess the cytotoxicity of blank films and Cly-loaded composite hydrogel films because they are a suitable cell line for in vitro cytotoxicity studies due to their important roles in wound healing, epithelial-mesenchymal interaction, and extracellular matrix development (Wong et al. 2007; Lee et al. 2020a, b). None of the films caused substantial cytotoxicity (> 82% viability) in L929 fibroblast cells, as shown in Fig. 5a, regardless of concentration. This demonstrated that Cly and the polymer released from the film are safe for topical application, particularly in situations (e.g., newborn tissues) where the safety of biomaterials is required (Hasan et al. 2019a, b).

Protein adsorption study

As shown in Fig. 5b, the adsorption of BSA onto the composite hydrogel film was relatively higher in SA-P-HA and Cly/SA-P-HA films compared to that in SA-P and Cly/SA-P films. The protein adsorption of SA-P, Cly/SA-P, SA-P-HA, and Cly/SA-P-HA films were 234.22, 188.88, 269.22, and 288.72 µg/cm^2, respectively. The percentage values were 1.17, 0.94, 1.85, and 1.44% for SA-P, Cly/SA-P, SA-P-HA, and Cly/SA-P-HA films, respectively. When foreign substances (e.g., wound dressings) come into contact with blood, protein uptake on the surface occurs, resulting in platelet activation and adhesion (Coleman et al. 1982). Thus,

when assessing platelet adhesion to artificial surfaces, the protein adsorption ratio is critical. Furthermore, the lower the number of adhered platelets, the higher the BSA adsorption ratio (Mohebali et al. 2020. Because of the addition of HA to the composite hydrogel films, the adsorption of BSA increased. Thus, the addition of polymers to composite films slightly affected the BSA adsorption ratios, implying that additional polymers in the composite films had little effect on platelet adhesion to artificial surfaces.

In vivo wound-healing activities and histological analysis

The wound-healing activity of Cly-loaded composite hydrogel films was evaluated in a mouse model of MRSA-infected wounds (Fig. 6). Because of the dorsal skin of a mouse is loose and elastic, it can reduce tension around wounds, speeding up wound contraction. Tegaderm™ was used to fix the skin and prevent skin contraction, thereby lessening the error resulting from wound contraction (Bae et al. 2012; Hlaing et al. 2018). Subsequently, wounds were treated with films daily based on their in vitro drug release profile, and an in vivo wound-healing assay was performed to determine whether Cly-loaded composite hydrogel films could accelerate the repair of MRSA-infected wounds by eradicating skin infection and promoting wound-healing. The measurement of wound area revealed that both Cly/SA-P and Cly/SA-P-HA film-treated groups showed greater eradication of skin infection and higher wound-healing activity than the untreated and blank films (SA-P and SA-P-HA). After day 5 post-injury, Cly/SA-P and Cly/SA-P-HA film-treated groups exhibited a progressive reduction in skin infection and enhanced wound healing. In contrast, the untreated and blank film (SA-P and SA-P-HA) groups showed no reduction in wound bacterial burden or wound healing (Fig. 6a). These findings confirmed that uncontrolled bacterial colonization of the wound surface and surrounding tissues could influence or delay the healing process from inflammation to remodeling. Accordingly, after reduction in the bacterial burden, the rate of healing significantly increased, with a reduction in the wound area from 56 to 29% (Cly/SA-P, $^{***}P < 0.001$) and 46 to 16% (Cly/SA-P-HA, $^{***}P < 0.001$) between days 5 and 7 post-injury (Fig. 6b). Importantly, treatment with Cly/SA-P-HA resulted in approximately complete wound closure (89% wound closure; $^{***}P < 0.001$) and clear re-epithelialization without any scab on day 9 post-injury (Fig. 6c), confirming the role of polymers used in the dressing to accelerate the healing process. We also observed the progress of skin healing in MRSA-infected wounds using H&E staining (Fig. 6d). The wound tissues from both the Cly/SA-P- and Cly/SA-P-HA film-treated groups significantly increased fibroblast-like cells and significantly decreased mononuclear inflammatory cells by day 9 post-injury. The healed skin structure was very similar to that of the healthy non-wounded skin. Furthermore, the untreated and blank film (SA-P and SA-P-HA) groups had open wounds with early epithelialization, ulceration, and an abundance of mononuclear inflammatory cells with deep inflammatory infiltration through the dermal layer.

The results suggested that the composite films from three mixed polymers (SA-P-HA) exhibited faster healing than the mixture of two polymers (SA-P). The combined healing effects of sodium alginate, pectin, and hyaluronic acid contributed to accelerated wound healing in MRSA-infected wounds. Sodium alginate promotes wound healing by regulating the formation of granulation tissues and enhancing the function of macrophages and pro-inflammatory cytokines (Paul et al. 2004; Yang et al. 2009). Pectin plays a role in enhanced healing by absorbing wound exudates, protecting against infection, and loading the drug/growth factors (Round et al. 2010; Munarin et al. 2012). Furthermore, hyaluronic acid modulates cell migration and proliferation (Toole 2004; Neuman et al. 2015). Therefore, in vivo wound healing results support the hypothesis that antibiotics incorporated into composite hydrogel films are able to remove infection and the composite (three mixed polymer) hydrogel films accelerate healing after MRSA infection is removed.

Conclusion

In this study, Cly-loaded composite hydrogel films were prepared, and their antibacterial and wound-healing activities were evaluated in MRSA-infected mice. Under immersed conditions, both the Cly/SA-P and Cly/SA-P–HA films exhibited drug release over 12 h. Both Cly/SA-P and Cly/SA-P-HA films showed potent antibacterial activity against MRSA (> 5 log reduction in bacterial viability). Furthermore, compared with the other groups, the Cly/SA-P-HA film-treated group significantly accelerated the healing and re-epithelialization of wounds in a mouse model of MRSA-infected wounds. None of the film dressings were toxic to healthy fibroblast cells. Thus, the Cly-loaded composite biopolymer films prepared in this study could be a promising wound dressing for treating infected cutaneous wounds.

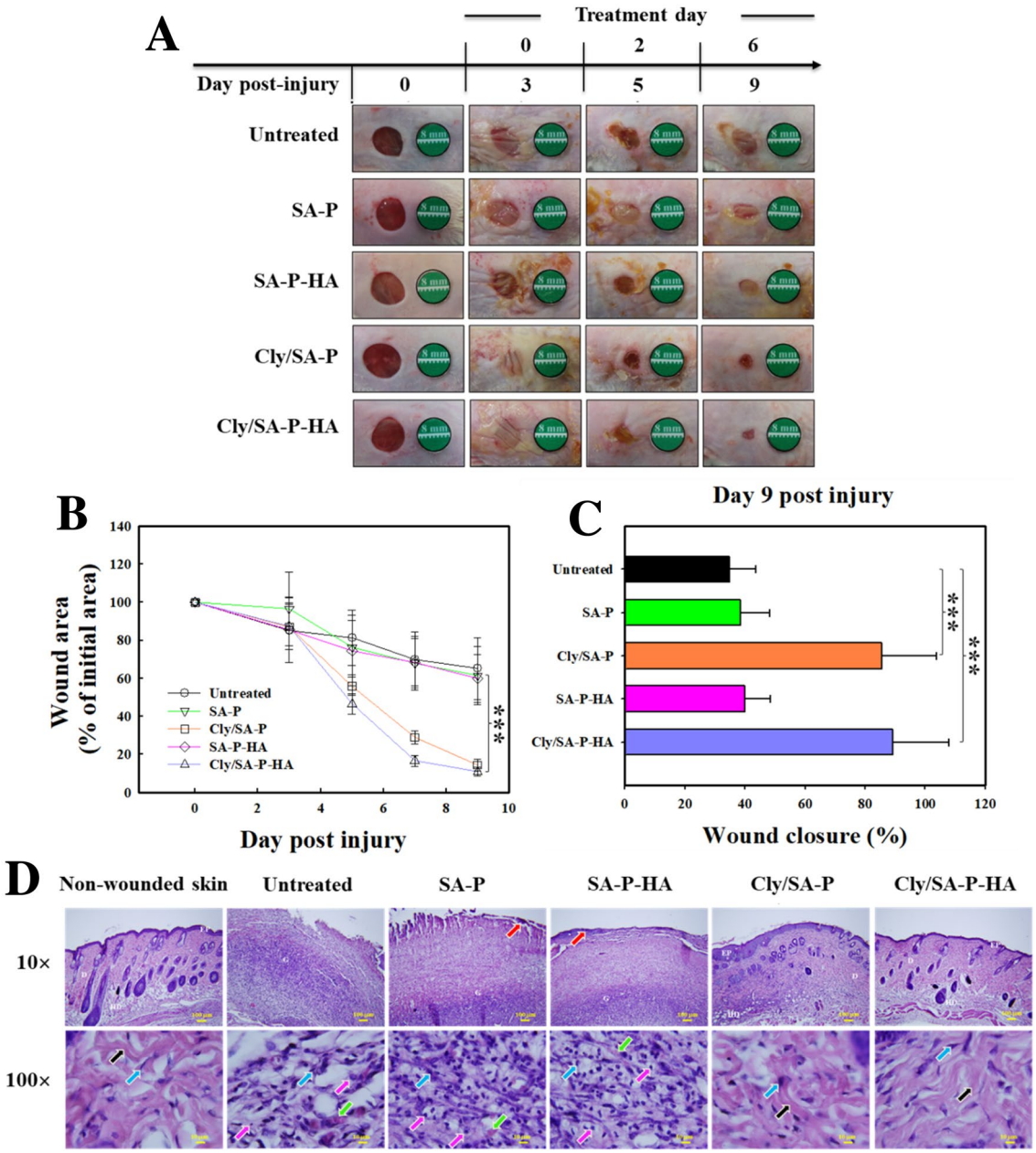

Fig. 6 Wound-healing assay in mice. **a** Representative photograph of MRSA-infected wounds of ICR mice treated with or without SA-P, Cly/SA-P, SA-P–H, and Cly/SA-P-HA films. **b** Area reduction (%) profiles of the wounds. Data are represented as means ± standard deviations, $n = 10$ different wounds, ***$P < 0.001$ compared with the untreated group. **c** Histological analysis (H&E staining) of MRSA-infected wounds of ICR mice at day 9. Scale bar = 100 µm. *Ep* epidermal, *D* dermal junction, *HD* hypodermis, and *G* granulation tissue. The red arrows indicate early epithelialization. Green arrows show capillaries (neovascularization), blue arrows indicate fibroblast cells, pink arrows denote mononuclear inflammatory cells, and black arrows show collagen strands

Acknowledgements This study was financially supported by the 2021 Post-Doc. Development Program of Pusan National University and the Basic Science Research Program through the National Research Foundation of Korea (NRF) funded by the Ministry of Education (No. NRF-2019R1I1A3A01057849).

Declarations

Conflict of interest All authors (N. Hasan, J. Cao, J. Lee, H. Kim, and J.-W. Yoo) declare that they have no conflict of interest.

Research involved in Human and Animal Rights All animal experiments were reviewed and approved by the Pusan National University Institutional Animal Care and Use Committee (PNU-IACUC) in 2020 (PNU-2020–2839).

References

Abou-Okeil A, Fahmy HM, El-Bisi MK, Ahmed-Farid OA (2018) Hyaluronic acid/Na-alginate films as topical bioactive wound dressings. Eur Polym J 109:101–109

Bae SH, Bae YC, Nam SB, Choi SJ (2012) A skin fixation method for decreasing the influence of wound contraction on wound healing in a rat model. Arch Plast Surg 39:457

Banna H, Hasan N, Lee J, Kim J, Cao J, Lee EH, Moon HR, Chung HY, Yoo J-W (2018) In vitro and in vivo evaluation of MHY908-loaded nanostructured lipid carriers for the topical treatment of hyperpigmentation. J Drug Deliv Sci Technol 48:457–465

Cao J, Su M, Hasan N, Lee J, Kwak D, Kim DY, Kim K, Lee EH, Jung JH, Yoo J-WJP (2020) Nitric oxide-releasing thermoresponsive pluronic F127/alginate hydrogel for enhanced antibacterial activity and accelerated healing of infected wounds. Pharmaceutics 12:926

Cho H-J (2020) Recent progresses in the development of hyaluronic acid-based nanosystems for tumor-targeted drug delivery and cancer imaging. J Pharm Investig 50:115–129

Choi M, Hasan N, Cao J, Lee J, Hlaing SP, Yoo J-W (2020) Chitosan-based nitric oxide-releasing dressing for anti-biofilm and in vivo healing activities in MRSA biofilm-infected wounds. Int J Biol Macromol 142:680–692

Coleman DL, Gregonis DE, Andrade JD (1982) Blood–materials interactions: the minimum interfacial free energy and the optimum polar/apolar ratio hypotheses. J Biomed Mater Res 16:381–398

Dou J-L, Jiang Y-W, Xie J-Q, Zhang X-G (2016) New is old, and old is new: recent advances in antibiotic-based, antibiotic-free and ethnomedical treatments against methicillin-resistant Staphylococcus aureus wound infections. Int J Mol Sci 17:617

Etxabide A, Vairo C, Santos-Vizcaino E, Guerrero P, Pedraz JL, Igartua M, De La Caba K, Hernandez RM (2017) Ultra thin hydro-films based on lactose-crosslinked fish gelatin for wound healing applications. Int J Pharm 530:455–467

Hasan N, Cao J, Lee J, Hlaing SP, Oshi MA, Naeem M, Ki M-H, Lee BL, Jung Y, Yoo J-W (2019a) Bacteria-targeted clindamycin loaded polymeric nanoparticles: effect of surface charge on nanoparticle adhesion to MRSA, antibacterial activity, and wound healing. Pharmaceutics 11:236

Hasan N, Cao J, Lee J, Naeem M, Hlaing SP, Kim J, Jung Y, Lee B-L, Yoo J-W (2019b) PEI/NONOates-doped PLGA nanoparticles for eradicating methicillin-resistant Staphylococcus aureus biofilm in diabetic wounds via binding to the biofilm matrix. Mater Sci Eng C 103:109741

Hasan N, Lee J, Kwak D, Kim H, Saparbayeva A, Ahn H-J, Yoon I-S, Kim M-S, Jung Y, Yoo J-W (2021) Diethylenetriamine/NONOate-doped alginate hydrogel with sustained nitric oxide release and minimal toxicity to accelerate healing of MRSA-infected wounds. Carbohydr Polym 270:118387

Hlaing SP, Kim J, Lee J, Hasan N, Cao J, Naeem M, Lee EH, Shin JH, Jung Y, Lee B-L (2018) S-Nitrosoglutathione loaded poly (lactic-co-glycolic acid) microparticles for prolonged nitric oxide release and enhanced healing of methicillin-resistant Staphylococcus aureus-infected wounds. Eur J Pharm Biopharm 132:94–102

Huanbutta K, Sittikijyothin W, Sangnim T (2020) Development of topical natural based film forming system loaded propolis from stingless bees for wound healing application. J Pharm Investig 50:625–634

Kim JO, Noh J-K, Thapa RK, Hasan N, Choi M, Kim JH, Lee J-H, Ku SK, Yoo J-W (2015) Nitric oxide-releasing chitosan film for enhanced antibacterial and in vivo wound-healing efficacy. Int J Biol Macromol 79:217–225

Kokabi M, Sirousazar M, Hassan ZMJEPJ (2007) PVA–clay nanocomposite hydrogels for wound dressing. Eur Polym J 43:773–781

Lamke LO, Nilsson GEA, Reithner HL (1977) The evaporative water loss from burns and the water-vapour permeability of grafts and artificial membranes used in the treatment of burns. Burns 3:159–165

Leaper DJ, Van Goor H, Reilly J, Petrosillo N, Geiss HK, Torres AJ, Berger A (2004) Surgical site infection–a European perspective of incidence and economic burden. Int Wound J 1:247–273

Lee KY, Mooney DJ (2012) Alginate: properties and biomedical applications. Prog Polym Sci 37:106–126

Lee J, Hlaing SP, Cao J, Hasan N, Ahn H-J, Song K-W, Yoo J-W (2019) In situ hydrogel-forming/nitric oxide-releasing wound dressing for enhanced antibacterial activity and healing in mice with infected wounds. Pharmaceutics 11:496

Lee J, Hlaing SP, Cao J, Hasan N, Yoo J-W (2020a) In vitro and in vivo evaluation of a novel nitric oxide-releasing ointment for the treatment of methicillin-resistant Staphylococcus aureus-infected wounds. J Pharm Investig 50(5):505–512

Lee J, Kwak D, Kim H, Kim J, Hlaing SP, Hasan N, Cao J, Yoo J-W (2020b) Nitric oxide-releasing s-nitrosoglutathione-conjugated poly (Lactic-Co-Glycolic Acid) nanoparticles for the treatment of MRSA-infected cutaneous wounds. Pharmaceutics 12:618

Li Y, Tian Y, Zheng W, Feng Y, Huang R, Shao J, Tang R, Wang P, Jia Y, Zhang J (2017) Composites of bacterial cellulose and small molecule-decorated gold nanoparticles for treating gram-negative bacteria-infected wounds. Small 13:1700130

Martínez-Aguilar G, Hammerman WA, Mason EO Jr, Kaplan SL (2003) Clindamycin treatment of invasive infections caused by community-acquired, methicillin-resistant and methicillin-susceptible Staphylococcus aureus in children. Pediatr Infect Dis J 22:593–599

Matthews KH, Stevens HNE, Auffret AD, Humphrey MJ, Eccleston GM (2005) Lyophilised wafers as a drug delivery system for wound healing containing methylcellulose as a viscosity modifier. Int J Pharm 289:51–62

Mohamad N, Amin MCIM, Pandey M, Ahmad N, Rajab NF (2014) Bacterial cellulose/acrylic acid hydrogel synthesized via electron beam irradiation: accelerated burn wound healing in an animal model. Carbohydr Polym 114:312–320

Mohebali A, Abdouss M (2020) Layered biocompatible pH-responsive antibacterial composite film based on HNT/PLGA/chitosan for controlled release of minocycline as burn wound dressing. Int J Biol Macromol 164:4193–4204

Moura LI, Dias AM, Carvalho E, De Sousa HC (2013) Recent advances on the development of wound dressings for diabetic foot ulcer treatment—A review. Acta Biomater 9:7093–7114

Munarin F, Tanzi MC, Petrini P (2012) Advances in biomedical applications of pectin gels. Int J Biol Macromol 51:681–689

Neuman MG, Nanau RM, Oruña-Sanchez L, Coto G (2015) Hyaluronic acid and wound healing. J Pharm Pharm Sci 18:53–60

Nurhasni H, Cao J, Choi M, Kim I, Lee BL, Jung Y, Yoo J-W (2015) Nitric oxide-releasing poly (lactic-co-glycolic acid)-polyethylenimine nanoparticles for prolonged nitric oxide release, antibacterial efficacy, and in vivo wound healing activity. Int J Nanomedicine 10:3065

Oshi MA, Naeem M, Bae J, Kim J, Lee J, Hasan N, Kim W, Im E, Jung Y, Yoo J-WJCP (2018) Colon-targeted dexamethasone microcrystals with pH-sensitive chitosan/alginate/Eudragit S

multilayers for the treatment of inflammatory bowel disease. Carbohydr Polym 198:434–442
Parris N, Coffin DR (1997) Composition factors affecting the water vapor permeability and tensile properties of hydrophilic zein films. J Agric Food Chem 45:1596–1599
Paul W, Sharma CP (2004) Chitosan and alginate wound dressings: a short review. Trends Biomater Artif Organs 18:18–23
Rezvanian M, Amin MCIM, Ng S-F (2016) Development and physicochemical characterization of alginate composite film loaded with simvastatin as a potential wound dressing. Carbohydr Polym 137:295–304
Round AN, Rigby NM, Macdougall AJ, Morris VJ (2010) A new view of pectin structure revealed by acid hydrolysis and atomic force microscopy. Carbohydr Res 345:487–497
Šiširak M, Zvizdić A, Hukić M (2010) Methicillin-resistant Staphylococcus aureus (MRSA) as a cause of nosocomial wound infections. Bosn J Basic Med Sci 10:32
Spížek J, Řezanka T (2004) Lincomycin, clindamycin and their applications. Appl Microbiol Biotechnol 64:455–464
Spížek J, Řezanka T (2017) Lincosamides: Chemical structure, biosynthesis, mechanism of action, resistance, and applications. Biochem Pharmacol 133:20–28
Stein M, Komerska J, Prizade M, Sheinberg B, Tasher D, Somekh E (2016) Clindamycin resistance among Staphylococcus aureus strains in Israel: implications for empirical treatment of skin and soft tissue infections. Int J Infect Dis 46:18–21
Thu H-E, Zulfakar MH, Ng S-F (2012) Alginate based bilayer hydrocolloid films as potential slow-release modern wound dressing. Int J Pharm 434:375–383
Toole BP (2004) Hyaluronan: from extracellular glue to pericellular cue. Nat Rev Cancer 4:528–539
Tsukada K (1992) The pH changes of pressure ulcers related headling process of wound. Wounds 4:16–20
Vivekanandan L, Sheik H, Singaravel S, Thangavel S (2020) Assessment of efficacy and safety of clindamycin against methicillin-resistant staphylococcus aureus (MRSA) infected subcutaneous abscess model. Antinfect Agents 18:144–151
Vowden K, Vowden P (2017) Wound Dressings: Principles and Practice Surgery (oxford) 35:489–494
Wang L, MaE A, Kerry JP (2010) Physical assessment of composite biodegradable films manufactured using whey protein isolate, gelatin and sodium alginate. J Food Eng 96:199–207
Wong T, Mcgrath JA, Navsaria H (2007) The role of fibroblasts in tissue engineering and regeneration. Br J Dermatol 156:1149–1155
Wynne R, Botti M, Stedman H, Holsworth L, Harinos M, Flavell O, Manterfield C (2004) Effect of three wound dressings on infection, healing comfort, and cost in patients with sternotomy wounds: a randomized trial. Chest 125:43–49
Yang D, Jones KS (2009) Effect of alginate on innate immune activation of macrophages. J Biomed Mater Res a 90:411–418